Automated Gas Chromatographic Method for Neutral Lipid Carbon Number Profiles in Marine Samples

Zheng Yang, Christopher C. Parrish*, and **Robert J. Helleur**

Ocean Sciences Centre and Department of Chemistry, Memorial University of Newfoundland, St. John's, Newfoundland, Canada A1C 5S7

Abstract

A gas chromatographic (GC) lipid-profiling method is optimized for analysis of neutral lipids in highly unsaturated marine samples. Chemometrics are employed to optimize autoinjection procedures and column temperature programs. The use of large solvent plug sizes, fast injection rates, hydrogen carrier gas with high flow rates, and short capillary columns enhanced recoveries of high molecular weight neutral lipids. A hydrogenation step was required to avoid discrimination of the flame ionization detector (FID) responses in highly unsaturated lipids. Analyses of fatty acids, which are moieties of the neutral lipids, support the neutral lipid profile data. The identification of major sterols is confirmed by gas chromatography with mass spectrometry (GC–MS). The values of summed molecular species from each neutral lipid class determined by GC are linearly correlated with neutral lipid subclasses determined by Chromarod thin-layer chromatography with flame ionization detection (TLC–FID). Automated high temperature GC on hydrogenated samples is found to offer a precise tool for the measurement of highly unsaturated neutral lipid compounds, which are critical in understanding physiological characteristics of cold water species. The method is applied to a range of marine samples including algae, bivalves, polychaetes, fish eggs, and fish larvae and reveals, for the first time, neutral lipid carbon number distributions in marine species from cold oceans.

Introduction

Neutral lipids, including tri-, di- and monoacylglycerols, sterols, steryl esters, hydrocarbons, wax esters, free fatty acids, and free aliphatic alcohols, are important components of marine food webs. For instance, triacylglycerols (TAG) constitute a major form of energy storage for marine plants and animals, and sterols regulate membrane functions and act as precursors for a range of metabolically active molecules. The composition of neutral lipid compounds, especially TAG, in marine animals can easily change through diet and other environmental factors. Certain ratios of neutral lipid subclasses, such as the ratio of TAG to sterols, may be useful as indices of physiological condition in marine animals (1).

The extremely complex nature and large number of molecular species with similar physico-chemical properties make chromatographic methods the exclusive way to profile lipids (2). Thin-layer chromatography with flame-ionization detection (TLC–FID), a high sample capacity, and simultaneous determination of both neutral and polar lipids has been used widely in the analysis of marine lipid subclasses (3), but some inherent limitations, such as insensitivity, nonlinear calibration curves, and slight variations between TLC rods, can restrict its usefulness (4,5). High-performance liquid chromatography (HPLC) has a great advantage over gas chromatography (GC) in the elimination of losses of temperature-sensitive unsaturated lipids and high molecular weight homologues. However, detection is less sensitive, there are more difficulties in identification, and analytical times are longer (6). Recently, supercritical fluid chromatography (SFC) has received a great deal of attention for lipid analyses because SFC can provide a wide range of operating conditions from gas-like separations similar to GC to liquid-like separations more comparable to HPLC. But analysis times with SFC are only shorter than those of HPLC, and co-elution of some important neutral lipid compounds is still unavoidable (7). GC provides, by far, the highest resolution of TAG based on carbon number in the shortest analytical time among the techniques mentioned (8). Moreover, GC is relatively sensitive and is readily automated, although its application is partially restricted to the more saturated low molecular weight species (9); it needs to be developed for the very long chain and highly unsaturated marine oils (10). Effects of the degree of unsaturation and losses of high molecular weight neutral lipid compounds in high temperature GC still pose problems.

In this study, the GC lipid-profiling method of Kuksis and coworkers (11,12) was optimized for use with neutral lipids in samples from cold marine environments, particularly those containing a high proportion of long chain polyunsaturated fatty acids (PUFA). Chemometrics were used to optimize autoinjection methods and the temperature programming of the column. Other components in the GC, including carrier gas types, injection techniques, length of the column, and septum

*Author to whom correspondence should be addressed.

types, were investigated. The importance of hydrogenation prior to GC analysis to minimize discrimination in highly unsaturated samples was also examined. The optimized high-temperature GC method was then applied to various plant and animal samples from the marine environment.

Experimental

Materials

The authentic neutral lipid mixtures employed in this study were prepared from chromatographically pure materials (at least 99% pure) supplied by Sigma (St. Louis, MO).

One species of bivalve, *Yoldia hyperborea,* and two species of polychaetes, *Nephthys ciliata* and *Artacama proboscidea*, were taken from the bottom of Conception Bay in Newfoundland, Canada. Larvae of cod (*Gadus morhua*) were obtained originally from the broodstock of Dalhousie University in Halifax, Nova Scotia, Canada (Scotian Shelf Cod). The remaining marine samples were cultured in the Ocean Sciences Centre of the Memorial University of Newfoundland. The flagellate, *Isochrysis galbana* (Clone T-iso), was grown in cage culture turbidostats. Fertilized eggs were obtained from two captive Atlantic halibut (*Hippoglossus hippoglossus*). Juvenile sea scallops (*Placopecten magellanicus*), fed differently cultured phytoplankton diets, were obtained from a pilot scale hatchery (OSC, St. John's, Newfoundland, Canada).

Extraction

One of the internal standards, tricaprin for neutral lipid profiles or *n*-hexadecan-3-one for TLC–FID analysis, was added to an aliquot of homogenized marine samples. The samples were extracted with a mixture of chloroform and methanol following the procedure of Bligh and Dyer (13).

Table I. Reduced Factorial Design, L_8 (2^7), in the First Experimental Block*

Method number	Plug size (µL)	Injection time (min)	Viscosity factor	Injection rate (µL/sec)	Injection ramp (°C/min)	T_{max} injection (°C)	Initial column temp. (°C)	Results (n = 2) Recovery† (M ± SD, %)	Resolution‡ (%)
1	0.5	0	2	1	100	340	62	21.8 ± 3.4	93
2	0.5	0	2	8	250	355	82	39.9 ± 2.9	83
3	0.5	1	4	1	100	355	82	33.8 ± 2.3	95
4	0.5	1	4	8	250	340	62	40.4 ± 1.5	53
5	2	0	4	1	250	340	82	37.6 ± 1.6	80
6	2	0	4	8	100	355	62	65.4 ± 3.8	50
7	2	1	2	1	250	355	62	45.1 ± 4.2	80
8	2	1	2	8	100	340	82	57.8 ± 6.0	75
9§	1	0	1	5	150	360	80	43.9 ± 4.3	90
CRV**	–1.40	–0.247	–0.253	–1.303	0.319	–0.533	0.319		

* Each compound at 5 ng per injection, helium carrier gas, a 5.5 m length of DB-5 column and a Thermolite septum; remaining conditions as in the experimental section.
† Recovery of 54:0 TAG compared with the internal standard, 30:0 TAG.
‡ Resolution between cholesteryl arachidate and 48:0 TAG (100% = complete baseline separation).
§ Manufacturer recommended method.
**Chromatographic response values.

Table II. Reduced Factorial Design of the Second Experimental Block*

Method number	Plug size (µL)	Injection time (min)	Viscosity factor	Injection rate (µL/sec)	Injection ramp (°C/min)	T_{max} injection (°C)	Recovery (mean ± SD, %)†
1	1	0	1	1	100	340	67.6 ± 2.1
2	1	0	1	5	200	360	75.8 ± 4.2
3	1	0.5	3	1	100	360	68.2 ± 3.6
4	1	0.5	3	5	200	340	72.7 ± 1.6
5	3	0	3	1	200	340	74.4 ± 1.6
6	3	0	3	5	100	360	88.1 ± 2.2
7	3	0.5	1	1	200	360	66.0 ± 0.4
8	3	0.5	1	5	100	340	87.4 ± 4.9
CRV	–0.635	0.235	–0.129	–0.959	0.449	0.079	

* Same conditions as those in (*) of Table I.
† Triplicate recovery of 54:0 TAG compared with the internal standard, 30:0 TAG, in a random injection sequence.

TLC–FID

Lipid classes in aliquots of the extracts were separated on silica gel-coated Chromarods-SIII (S.P.E. Ltd., Concord, Ontario, Canada) using four different solvent systems and measured in an Iatroscan MK V (S.P.E. Ltd.) after development with each solvent system (14).

Column chromatography

An aliquot of total lipid chloroform extract from marine samples was passed through a pasteur pipette containing 0.2 g Florisil (Fisher Scientific, Springfield, NJ). The neutral lipid fraction was eluted with 8 mL of chloroform–methanol–formic acid (99:1:1, v/v/v).

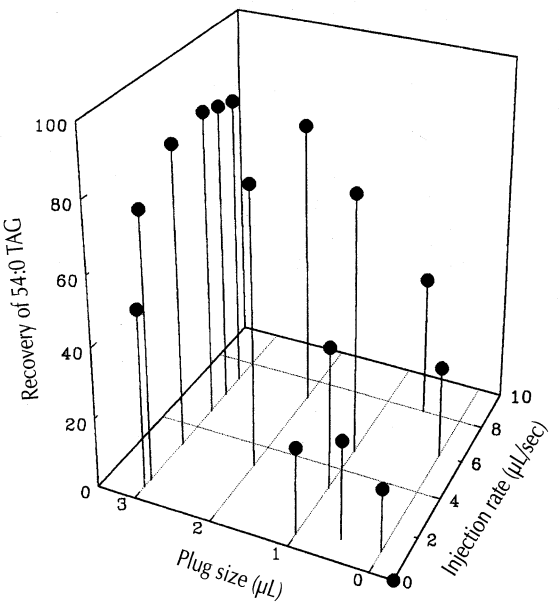

Figure 1. Response–surface plot of recovery of tristearin (54:0 TAG) versus solvent plug size and injection rate (helium carrier gas, 5.5-m DB-5 column, and Thermolite septum, remaining conditions in experimental section).

Hydrogenation

An aliquot of each neutral lipid chloroform fraction and 5 mg fresh platinum oxide (Sigma) were placed in a 10-mL vial and bubbled with a gentle flow of hydrogen gas for 20 min without stirring. The hydrogen-filled vial was capped, sealed, and then stirred vigorously with a magnetic stirrer for 2 h. The hydrogenated sample was then filtered to remove the catalyst. In addition, most samples were also hydrogenated by means of an atmospheric pressure hydrogenator in semi-micro scale (15) to check the efficiency of the simpler method.

Derivatization

Trimethylsilylation (TMS)

An aliquot of dried neutral lipid fraction was mixed with one drop of *N,O*-bis(trimethylsilyl)-acetamide and two drops of *N,O*-bis(trimethylsilyl)-trifluoroacetamide (Pierce, Rockford, IL), then heated at 70°C for 15 min. The TMS derivative was diluted with chloroform prior to GC analysis.

Fatty acid methyl esters (FAME)

An aliquot of the neutral lipid fraction was derivatized to FAME using 14% of a BF_3–methanol solution (Pierce). The sample and 2 mL of methylating reagent were heated at 80°C for 1 h. One mL of doubly distilled water was added, followed by 4 mL of hexane. The FAME were obtained by withdrawing the organic phase after centrifuging the mixture at 1000 rpm for 5 min.

Gas chromatography

Neutral lipid profiles were investigated using a model 3400 Varian GC equipped with a model 8100 autosampler, a model 1093 septum-equipped programmable injector with a high-performance insert, and an FID (Varian, Walnut Creek, CA). The analytical column was a flexible fused-silica column (0.32-mm i.d., 0.25-µm film thickness) that was coated with cross-linked 5% phenylmethyl silicone (J&W Scientific, Folsom, CA). The carrier gas (helium) flow was set at 10 psi of the column head pressure. The flow rate of the fuel gas (hydrogen) was adjusted to 30 mL/min, and the air flow was set at 300 mL/min. The temperature of the FID was 345°C. The column temperature was programmed to rise from the initial temperature to 115°C at 40°C/min, to 225°C at 25°C/min, to 280°C at 15°C/min, and to the final temperature, 340°C, at 5°C/min, and then to hold for 4 min. The parameters for autoinjection, the injection temperature program, initial column temperature, type of carrier gas, injection technique, length of the column, and septum types in the GC were optimized in this study. Data acquisition, baseline subtraction, quantification, and chromatogram replotting were processed with Varian GC Star Workstation software.

FAME analyses were carried out with the same GC model using a flexible fused-silica column (30 m × 0.32-mm i.d.) coated with Omegawax 320 (Supelco, Bellefonte, PA).

Table III. Comparison of Carrier Gas Flow Rates and Retention Times for 54:0 and 60:0 TAG on a DB-5 Column (5.5 m × 0.32-mm i.d.)*

Gas pressure (psi)†	Flow rate (mL/min)‡		Retention time (min)				Resolution§	
			H_2		He			
	H_2	He	54:0	60:0	54:0	60:0	H_2	He
12	23.1	16.7	17.81 ± 0.04	21.54 ± 0.08			90	
10	21.0	12.5	18.41 ± 0.04	22.20 ± 0.06	22.20	28.90	95	70
8	17.6	9.38	19.51 ± 0.08	23.63 ± 0.08			95	
6	14.0	6.25	20.43 ± 0.04	**			90	
4	8.63	3.45	22.02 ± 0.09	**			80	

* $n \geq 2$, each compound at 5 ng per injection, and at optimized conditions: 3 µL chloroform solvent plug, 5 µL/sec injection rate, 0.0 min injection time, viscosity factor 2, 100°C/min injection ramp, 355°C maximum injection temperature, 61°C initial column temperature, and Thermolite septum.
† Carrier gas pressure at the column head.
‡ Measured at ambient temperature.
§ Resolution between cholesteryl arachidate and 48:0 TAG (100% = complete baseline separation).
**Retention time of 60:0 TAG > 25 min.

The gases and flow rates were the same as those for the neutral lipid profiles. The injection temperature was programmed to rise from 65°C to 250°C at 200°C/min and then to hold for 0.10 min at 250°C. The column temperature was programmed to rise from 70°C to 195°C at 40°C/min, to hold for 8 min at 195°C, and then to rise to 240°C at 3°C/min, and finally to hold for 5.4 min at 240°C. The temperature of the FID was kept at 260°C. Peaks were identified by comparing their retention times with those of FAME standards: menhaden oil, PUFA-1 and PUFA-2 FAME mixtures (Supelco Canada, Oakville, Ontario, Canada), and 13:0–21:0 and 20:0–20:4 pure FAME (Alltech, Deerfield, IL).

Gas chromatography–mass spectrometry

Some of the identities of the methylsilylated neutral lipid compounds (i.e., sterols) were confirmed with a Hewlett-Packard 5890/5971A gas chromatograph–mass spectrometer (GC–MS) using 70-eV electron impact ionization over the mass scanning range of *m/z* 35–650. The mass detector temperature was 260°C. Methylsilylated compounds were separated on the same type of column as the above neutral lipid profiles except that it had an inner diameter of 0.25 mm. Following manual on-column injection at 150°C, the column temperature was programmed to rise to 275°C at 10°C/min, to 310°C at 4°C/min, to 340°C at 2°C/min, and then to hold for 3 min at 340°C.

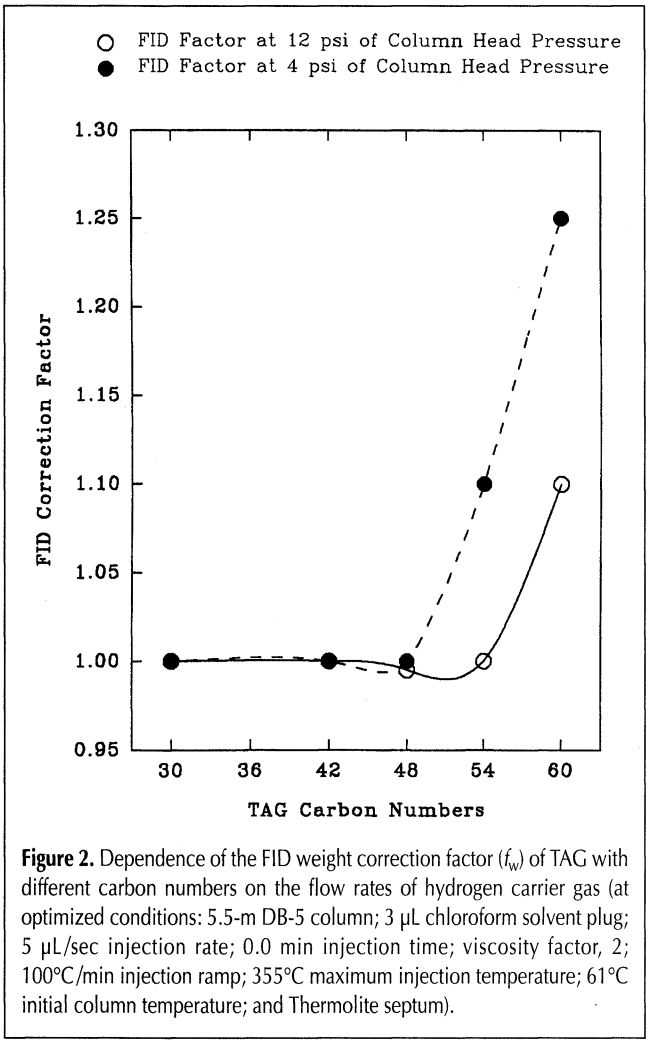

Figure 2. Dependence of the FID weight correction factor (f_w) of TAG with different carbon numbers on the flow rates of hydrogen carrier gas (at optimized conditions: 5.5-m DB-5 column; 3 µL chloroform solvent plug; 5 µL/sec injection rate; 0.0 min injection time; viscosity factor, 2; 100°C/min injection ramp; 355°C maximum injection temperature; 61°C initial column temperature; and Thermolite septum).

Multivariate method

A two-level multivariate analysis, Latin Square L_8 (2^7), was used to screen a number of potentially important variables in the autosampler as well as in the injection temperature program and the initial column temperature. As shown in Table I, L_8 (2^7) means that seven variables were scanned in eight runs, each at two levels. The factor values at low and high levels were selected based on the literature; 0.3 of the full range of the variables was selected as the low level, and 0.7 of the full range was the high level. The changes of factors were run independently, allowing uncorrelated parameter estimation. Method 9 in Table I involves the parameters recommended by the manufacturer, Varian.

Two responses were selected to measure chromatographic behavior. The primary response was the relative recovery of 54:0 TAG, which was a predominant acyl carbon number in most marine samples. A second factor was the resolution between cholesteryl arachidate and tripalmitin (48:0 TAG), two closely eluted compounds in the chromatogram. A higher recovery of long-chain TAG is usually taken to be more important than the separation efficiency in analysis of natural lipid mixtures. The prime response values were evaluated with the following equation:

$$CRV = \Sigma(L_i) - \Sigma(H_i)$$

where CRV represents the chromatographic response values, L_i is the recovery of 54:0 TAG at the low level of the variable i, and

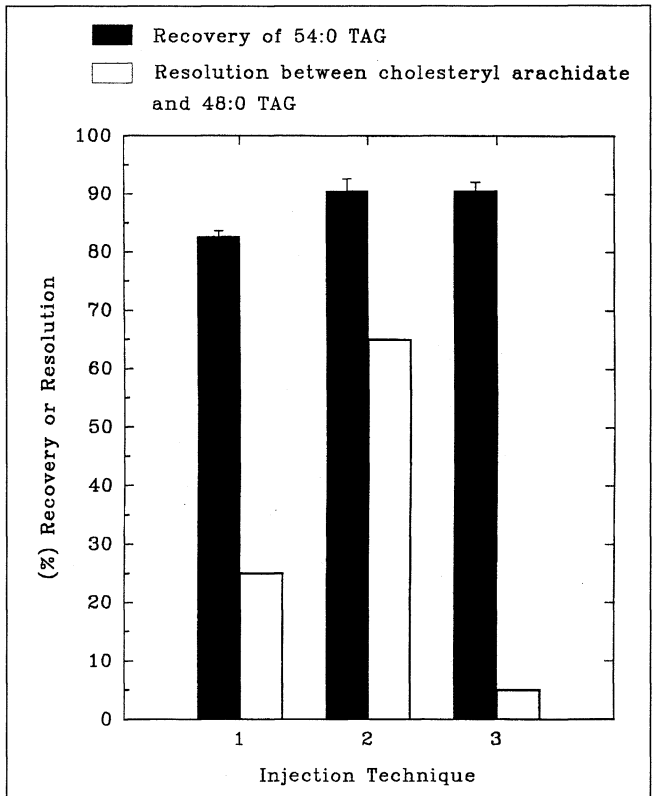

Figure 3. Influence of injection technique on recovery and resolution at optimized GC conditions (1, autoinjection; 2, manual with lower air gap; and 3, manual solvent flush injection; mean ± standard deviation, $n \geq 3$ at optimized conditions as listed in Figure 2 with helium as the carrier gas).

H_i is the same recovery at the high level of the same variable *i*. Positive values meant that the low level was better; negative values meant that the high level was better. Large absolute CRV suggested that this variable was more important and significantly affected the recovery of 54:0 TAG.

In the second experiment (Table II), the better points of each variable in the previous run served as the central value. New values of the two-level analyses were selected from the middle points between the better points in the previous analysis and the limits of these variables, and from the middle points between the better and worse points in the last run. Finally, the response–surface method was employed to locate the optimum over the major experimental variables.

Results and Discussion

Optimization of autoinjection

The transfer of the liquid sample from the syringe needle to the internal wall of the column is a crucial step in obtaining a high degree of accuracy and precision because of the high molecular weight of TAG and the corresponding high temperatures required for GC elution. Factorial design offers very effective coverage of the experimental domain in comparatively few experiments. By varying all of the experimental factors simultaneously, the main effects of the variables and the potential interactions can be determined (16).

Absolute CRV calculated in Tables I and II show that the order of importance is: injection rate ≥ plug size >> injection ramp > maximum temperature of injector > injection time ≈ solvent viscosity factor ≥ initial temperature of the column.

The autosampler injection rate and the solvent plug size appeared to be critical in increasing the recovery of 54:0 TAG. The optimum, which was the apex of the response surface of recovery of 54:0 TAG (the recovery rather than CRV was used for a direct comparison) over these two experimental domains, was located at 3 µL plug size and 5 µL/sec injection rate, as illustrated in Figure 1. A rapid injection pushes most of the sample into the column or the insert of the GC and eliminates the possibility of sample "coating" the outside of the needle. In addition, a slow injection leaves some liquid hanging at the needle tip. As a consequence, a greater proportion of high-boiling compounds remains on the withdrawn needle with slow injection, causing discrimination against high molecular weight TAG (17). A similar result was obtained by Grob et al. (18) with alkanes. Large solvent plugs probably flush most of the remaining viscous neutral lipid compounds from the needle to the column and serve as a wall to protect against possible backflushing of the sample in the column or insert during the rapid increase of column temperature. Large plug sizes also enlarge the peak area of 54:0 TAG and give smaller standard deviations. The peak area of 54:0 TAG almost doubles with a change in plug size from 0 to 3 µL; however, this advantage is accompanied by a decrease in the resolution between cholesteryl arachidate and 48:0 TAG.

It should be noted that interactions between most variables are insignificant. Only the injection rate and plug size showed a definite co-effect on the recovery of 54:0 TAG. CRV of summed same levels in both predominant variables $[(H \times H) + (L \times L)]$ were greater than that of summed different levels $[(H \times L) + (L \times H)]$. The entire sequence for these two variables from the most significant to insignificant was $H \times H > H \times L$ or $L \times H > L \times L$. This was quite predictable. A rapid injection not only eliminates sample filming on the outside of the needle but also forces the solvent plug behind the air gap and the sample segment to spray from the syringe to the column to flush out any lipids remaining in the syringe. Both functions enhance recovery of high molecular weight compounds.

Other parameters also improved chromatographic performance at certain levels. The rate of the injector temperature program influenced CRV second only to the effects of the solvent plug and injection rate (Tables I and II). The rate at 100°C/min achieved much better results than at either 200 or 250°C/min. This rate created a speed of evaporation that was faster than the column ramp to transfer a sharp component band to the column but not so fast as to yield wild evaporation and to produce a flashback from the column.

The initial injector temperature, like the initial column temperature, was set close to the boiling point of the solvent to let the entire sample deposit on the column in liquid form. The final injection temperature was set at 15°C above the maximum column temperature. This achieved higher 54:0 TAG recovery because the top of the injector, which includes the septum, is cooler than the main body of the injector. A higher temperature for the injector prevents high-boiling components from recondensing in a relatively cool injector head.

The initial temperature of the column was tested to determine if solvent- or solute-focusing techniques were better. Setting the temperature slightly below the solvent boiling point allowed higher recovery of 54:0 TAG, shortened the interval between two analyses, and avoided possible phase stripping in the front coils of the column as compared to the solute-focusing technique. After a rapid injection, which deposits samples onto the column or the insert of the injector, a column temperature near the boiling point of the solvent produces sufficiently slow evaporation to avoid violent backflow. On the other hand, solute focusing with rapid

Table IV. Recovery and Retention Time of Tristearin (54:0 TAG) with Respect to the Column Length*

Length of DB-5 Column (m)	8.6	8.1	7.5	5.5
Recovery of 54:0 TAG (mean ± SD, %)	–	71.9 ± 3.9	89.2 ± 2.1	90.7 ± 2.5
Retention time of 54:0 TAG (min)	not eluted after holding column at 340°C for 14 min	32.1	25.7	22.2

* Minimum of 3 injections each of 10 ng under optimized conditions (as in [*] of Table III) for each length of the column; helium as the carrier gas.

solvent evaporation cannot transport all the sample vapor through the carrier gas flow because the initial column temperature is 10–20°C above the boiling point of the solvent. Excessively high sampling temperatures at both the injector and the column cause difficulties in the fast and complete transfer of samples into the column and decrease the column resolution as well as the precision and accuracy of quantitative analyses (19).

Reducing the dwell time of the syringe needle in the injector inlet from 1 min to 0.5 min, then to 0 min, slightly increased 54:0 TAG recovery as the short dwell time prevented needle heating and associated needle discrimination problems. Similarly, Klee (20) found that longer needle dwell times were associated with smaller peak areas as carbon numbers of *n*-alkanes increased. These observations can be explained by assuming that some time is needed to build up an effective backflow (21).

Injection volume is also important when obtaining reproducible, undiscriminated data. Injection volumes that are too small not only yield large standard deviations between injections but also reduce the speed of the liquid at the needle tip. However, backflow through the column entrance and the possibility of shortening column lifetimes may be problems with large injection volumes (21). Comparison of different injection volumes showed that a volume of 1 µL was the most suitable.

Carrier gases

Hydrogen carrier gas provides superior efficiency over a larger linear velocity range, and its optimum linear velocity is much higher in comparison with helium (Table III). At the same column head pressure, the retention times of high molecular weight TAG, such as 54:0 and 60:0 TAG, decreased 20–30% with hydrogen carrier gas as compared to helium, so that unstable high molecular weight lipids had less chance of decomposing during GC analysis. Furthermore, the higher optimum flow rate of hydrogen maintained a similar resolution to that achieved by helium at a lower flow rate. Overall, analysis time can be shortened and column lifetime can be prolonged by using hydrogen as the carrier gas.

The flow rate also plays an essential role in optimizing GC performance. The data with hydrogen carrier gas set at 12 and 4 psi of column head pressure showed that there was no difference in the FID response at the low TAG carbon number range, C_{30}–C_{48}, but higher flow rates definitely minimized discrimination in the FID responses for higher carbon number TAG (Figure 2). This

Table V. Evaluation of Six Kinds of Septums Used in the Injection Port*

Septum	T_{max} (°C)	Relative recovery of 54:0 TAG (mean ± SD, %)	Nature of chromatogram
Thermolite†	340	89.1 ± 3.1	clean baseline
77 HT‡	400	75.9 ± 8.4	clean baseline
Red HT‡	400	75.6 ± 4.2	clean baseline
Blue‡	350	74.4 ± 7.0	clean baseline
Thermogreen§	300	89.1 ± 2.5	rough baseline at beginning
White**	?		peaks split; "ghost" peaks present

* With helium as the carrier gas and 3 injections under optimized method with each kind of septum.
† Septum from Restek, Bellefonte, PA.
‡ Septa from Chromatographic Specialties, Inc., Brockille, ON, Canada.
§ Septum from Supelco, Inc.
**Septum from Varian, Inc., Sugar Land, TX.

Table VI. Reproducibility of Relative Retention Times and Peak Areas, and Measurements of FID Weight Correction Factor (f_w)*

Lipid compounds	Carbon number†	Retention time (min)	Peak area	C.V. of peak area (%)‡	Relative weights	f_w§
Octodecane	C_{18} HC	3.236 ± 0.007	3735 ± 43	1.151	1.089	0.776
Nonadecane	C_{19} HC	3.634 ± 0.006	3913 ± 133	3.399	1.062	0.772
Palmitic acid	C_{16} FA	4.214 ± 0.007	3870 ± 101	2.610	1.011	0.695
Stearic acid	C_{18} FA	4.919 ± 0.006	3663 ± 154	4.204	0.989	0.719
Cholesterol	C_{27} ST	7.968 ± 0.009	4219 ± 20	0.474	1.033	0.652
Campesterol	C_{28} ST	8.366 ± 0.009	3558 ± 17	0.478	0.834	0.623
Sitosterol	C_{29} ST	8.701 ± 0.010	4564 ± 69	1.502	1.034	0.603
Tricaprin	30:0 TAG	9.450 ± 0.012	2661 ± 69	2.602	1.000	1.000
Stearic acid stearyl ester	C_{36} WE	10.45 ± 0.014	2804 ± 148	5.293	0.986	0.936
Cholesteryl palmitate	C_{43} SE	16.95 ± 0.026	2923 ± 69	2.360	1.017	0.926
Cholesteryl stearate	C_{45} SE	18.54 ± 0.026	2663 ± 44	1.646	0.939	0.938
Cholesteryl arachidate	C_{47} SE	20.11 ± 0.027	2320 ± 198	8.527	0.959	1.100
Tripalmitin	48:0 TAG	20.36 ± 0.027	2775 ± 47	1.707	0.952	0.913
Tristearin	54:0 TAG	25.52 ± 0.045	2159 ± 80	3.703	0.995	1.226

* 5 consecutive runs at the optimized conditions (as those in [*] of Table III) compared with an internal standard, 30:0 TAG, each compound at 5 ng per injection, and with helium as the carrier gas.
† Carbon numbers in hydrocarbons (HC), fatty acids (FA), sterols (ST), wax esters (WE) , and steryl esters (SE) are summed carbon numbers; in triacylglycerols (TAG) summed acyl carbon numbers are used.
‡ C.V. = coefficient of variation
§ Peak area/weight, relative to tricaprin.

observation confirms those of Mares et al. (22) with hydrogen carrier gas and Hinshaw et al. (23) with helium.

The possibility of an explosion is a major concern using hydrogen carrier gas, especially if the GC is left running automatically overnight. As the explosive threshold for hydrogen in air is 4%, keeping the fume hood fan working and regularly checking for leaks should prevent any potential accidents. However, for reasons of safety, helium carrier gas was used primarily in this study.

Optimization of other GC parameters

Certain other GC parameters were also optimized as follows. Manual injection is required for the analysis of trace amounts of lipids when there is not sufficient material for an autosampler to remove a sample from the vial (minimum volume is 0.4 mL per sample). Compared to autoinjection, manual injection methods exhibited slightly higher recoveries of 54:0 TAG (Figure 3). However, resolution of cholesteryl arachidate and 48:0 TAG was very different. The reason may be that manual solvent flush injection (method 3 in Figure 3) cannot inject as quickly as the autoinjector, allowing the solute to migrate in a relatively greater solvent matrix and making the peaks wider. Manual injection without the solvent plug (method 2 in Figure 3) resulted in the best resolution. However, as mentioned above, injection without a solvent plug led to the smallest peak size and the highest standard deviation.

The suitable column length was tested under optimized conditions; helium was used as the carrier gas. In reference to recovery of 54:0 TAG, durability of the column, and resolution in chromatograms, a column length of 5.5 m is ideal (Table IV). Higher elution temperature and increased residence time in the chromatographic system can lead to possible polymerization and decomposition of high molecular weight neutral lipids and result in their disappearance or lowered recoveries (6). Both factors increase with column length so that the shortest column that still provides acceptable resolution of sample components is best.

Differences in recovery of 54:0 TAG and the backgrounds of chromatograms with different septum types in the injector may result from different sealing statuses in subsequent injections (Table V). Higher temperature limits of the septum coincide with harder septum materials, which leads to weaker sealing ability. Thermolite (Restek, Bellefonte, PA) displayed the best performance among the six kinds of tested septums.

Influence of lipid composition on chromatograms

Interferences from overlap of individual neutral lipid compounds have been carefully studied. TAG are a main group of neutral lipids in most marine samples. TAG with acyl carbon numbers over 49 are usually the sole lipid components at the high temperature region during GC analysis. However, the C_{48} TAG peak may overlap with that of cholesteryl arachidate if both are major compounds, as is the case for lipids isolated from marine species. Their chromatographic resolution has been selected as a critical objective in evaluating GC performance. Generally, hydrogen carrier gas achieved better resolution than helium for this pair of compounds.

A small proportion of TAG may have carbon numbers below 48. These TAG are commonly found to have even carbon numbers down to 34 or so, but do not reach C_{30} in most samples. These minor compounds may interfere in the determination of cholesteryl esters with carbon numbers 47 or 45. In most cases, the concentrations of these low carbon number TAG are sufficiently low, so their effect on the determination of cholesteryl esters is negligible; however, a few marine samples are rich in low carbon number TAG (24). Such a significant interference for cholesteryl esters can be resolved by prehydrogenation of samples, which enables good separation of C_{47} cholesteryl ester from C_{46} TAG (25). After establishing that there were no detectable TAG with carbon numbers over 62 in the marine samples analyzed, GC analyses were ended at the retention time of C_{63} TAG to prolong the column life.

Wax esters, found in abundance in some marine species (26), may cause an overlap at the lower temperature side of the chromatogram. For instance, the internal standard, tricaprin, may overlap with palmitic acid stearyl ester. This problem can be avoided by prior scanning for potential interferences with tricaprin.

Precision and linear ranges

Quantitative analysis requires not only independence of FID weight correction factors (f_W) from the composition and size of

Table VII. FID Weight Correction Factor (f_w) of Typical Neutral Lipid Subclasses Versus Individual Amounts Per Injection*

	Amounts (ng, n = 3)				
Neutral lipid compounds	0.1	1	10	100	500
Octadecane	1.601 ± 0.899	0.961 ± 0.094	0.757 ± 0.035	0.716 ± 0.029	0.704 ± 0.002
Palmitic acid	0.931 ± 0.024	0.842 ± 0.069	0.749 ± 0.032	0.718 ± 0.031	0.713 ± 0.013
Monopalmitin	1.101 ± 0.123	0.629 ± 0.168	0.729 ± 0.033	0.716 ± 0.030	0.724 ± 0.013
Cholesterol	0.667 ± 0.254	0.753 ± 0.172	0.666 ± 0.030	0.679 ± 0.028	0.677 ± 0.014
Tricaprin (30:0 TAG)	1.000 ± 0.149	1.000 ± 0.025	1.000 ± 0.043	1.000 ± 0.043	1.000 ± 0.022
Stearic acid stearyl ester	1.426 ± 0.490	0.986 ± 0.248	0.922 ± 0.097	0.845 ± 0.043	0.836 ± 0.018
Dipalmitin	0.453 ± 0.095	0.741 ± 0.036	0.915 ± 0.045	0.883 ± 0.083	0.851 ± 0.019
Cholesteryl stearate	0.706 ± 0.264	0.846 ± 0.088	0.959 ± 0.048	0.932 ± 0.042	0.903 ± 0.021
Tripalmitin	0.663 ± 0.290	0.969 ± 0.232	1.061 ± 0.045	1.013 ± 0.042	0.993 ± 0.023
Tristearin	1.000 ± 0.199	1.255 ± 0.106	1.283 ± 0.057	1.187 ± 0.046	1.152 ± 0.028

* At optimized conditions (as in [*] of Table III) and with helium as the carrier gas.

neutral lipid compounds, but also reproducibility of the measurement over wide ranges of concentration. Precision of the optimized method can be seen from a repeated sequence of measurements made by using a mainly saturated synthetic mixture which represented most neutral lipid subclasses in marine samples (Table VI). With helium carrier gas and a sample load of 5 ng per compound, the relative standard deviation of peak areas for most standards was below 5%. Only cholesteryl arachidate showed a somewhat larger variation (8.5%) due to partial overlap with 48:0 TAG. The f_W values ranged from 0.6 for most sterols to 1.2 for 54:0 TAG, compared to the internal standard, 30:0 TAG. These were comparable with published data (11). With a 28-min run and by using an autosampler, over 40 injections could be accomplished in 24 h. Therefore, this method is relatively precise and rapid.

Values of f_W can depend on the sample size and on the absolute amounts of the neutral lipid compounds in the injected samples. Table VII shows that the linear ranges of each neutral lipid compound under optimized conditions encompassed almost three orders of magnitude. The detection limits of most compounds reached 0.01 ng per compound, which is about three orders of magnitude lower than those of TLC–FID. However, linear ranges only reached 1 ng per compound for most tested neutral lipid subclasses. At 0.1 ng per compound, their f_W changed by 25% to 75% of the values in their linear range. The maximum loading amount was up to 400–500 ng per compound. Above that, peak tailing significantly decreased the resolution between adjacent peaks.

It is possible to calculate the expected FID response factors by using the effective carbon number concept (27). Most of the values in Table VI and in the last column of Table VII are within 10% of the theoretical value. The largest discrepancies occurred at the highest carbon number value, which presumably resulted from tristearin loss at the higher elution temperature.

The role of hydrogenation

Model systems that are optimized on mainly saturated neutral lipids are unable to match all molecular species in real samples, particularly when the samples contain a high percentage of various long-chain PUFA, which are common in samples from subpolar marine environments. The chromatographic behavior of highly unsaturated neutral lipids in high temperature GC could be inconsistent with those of saturated or monounsaturated homologues. Most systematic GC studies have omitted the effect of unsaturation. Mares et al. (22,28) optimized GC conditions without examining hydrogenation in the analysis of intact long-chain TAG. They used both short, nonpolar capillary columns and packed columns and optimized a range of parameters. Only saturated TAG with different chain lengths were employed in their model mixtures, probably because of the small proportions of long-chain PUFA in their biological samples. Subsequently, Mares (29) explained that higher f_W values were used to compensate for losses of unsaturated lipids. However, the diverse levels of unsaturation in neutral lipids with the same carbon numbers suggest that there could be great differences in their f_W values.

Discrimination according to the degree of unsaturation on the recoveries of TAG was observed with standards using either

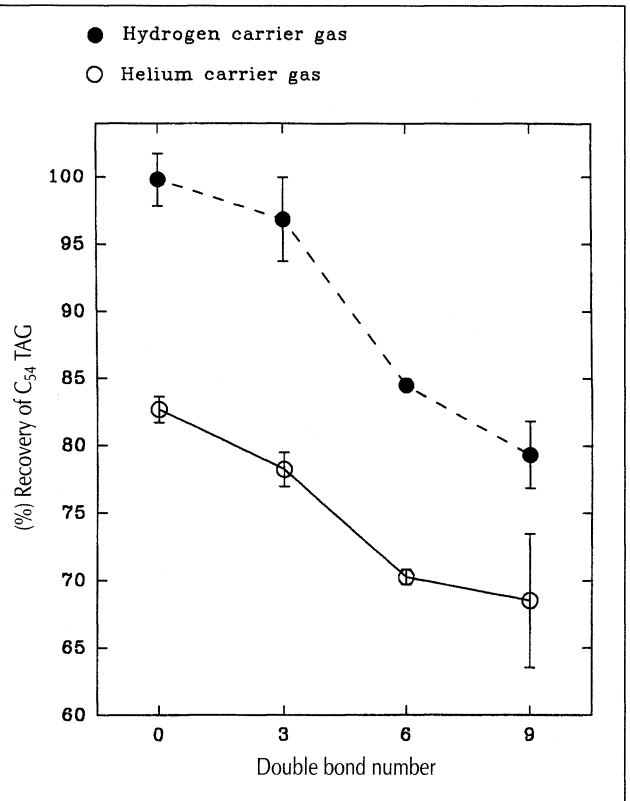

Figure 4. Relative recovery of synthetic C_{54} triacylglycerols in relation to the degree of unsaturation (mean ± standard deviation, $n = 3$, at optimized conditions as listed in Figure 2).

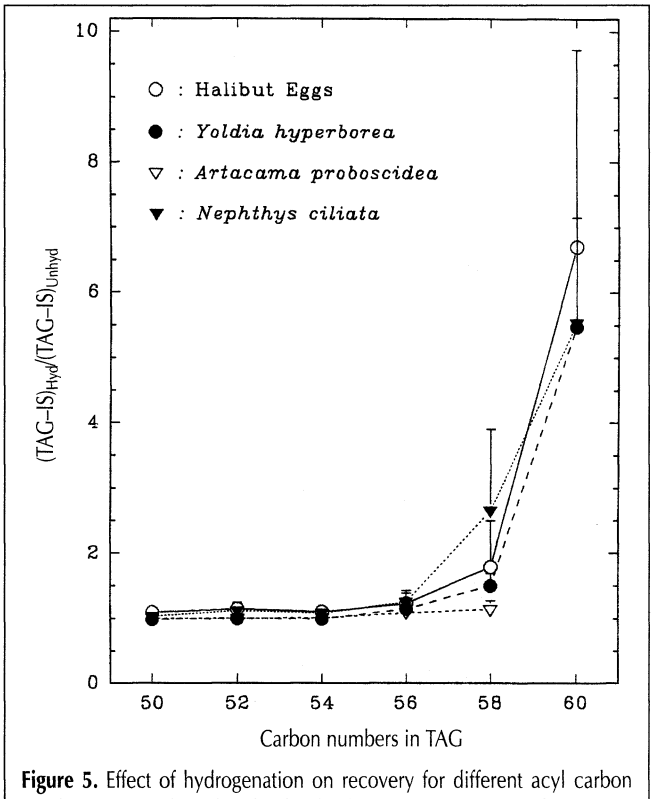

Figure 5. Effect of hydrogenation on recovery for different acyl carbon numbers in TAG from four kinds of cold water marine animals (mean ± standard deviation, $n \geq 3$, at optimized conditions as listed in Figure 2 with helium as the carrier gas).

hydrogen or helium as the carrier gas (Figure 4). An increase in the number of double bonds accompanied a decline in recoveries of TAG with the same carbon number, C_{54}. Recoveries of highly unsaturated TAG were not very reproducible with helium as a carrier gas, presumably because of the longer period at high temperature (Table III). Gilkison (30) observed a similar result with helium carrier gas and a polar stationary phase, 65% phenylmethyl silicone. Losses of unsaturated TAG may not be reproducible when there are over six double bonds in a TAG molecule or when the number of double bonds in an individual acyl group is greater than three (6).

This recovery problem was even more serious in lipids from actual cold water samples. In Figure 5, the *y*-axis shows the ratios of hydrogenated to unhydrogenated samples, each divided by the peak area of the internal standard, 30:0 TAG. At the lower carbon number range, 50–56, the ratios were near one, but at the higher carbon number region, a steep increase of ratios with larger standard deviations was observed. Mares et al. (25) found that the amounts of TAG with higher carbon numbers, such as 56 and 58, were significantly different before and after hydrogenation. Their biological samples did not contain TAG with carbon numbers of 60 or higher, and their mean carbon numbers were lower compared to these samples from a cold ocean environment. They concluded that differences in recoveries of high molecular weight TAG with respect to hydrogenation had only a small influence on the recovery of the total TAG. Here, the mean carbon numbers of TAG in the cold ocean animals ranged from 52 to 56, which indicated that about 50% or more TAG had carbon numbers greater than 54. This implied that the animals probably accumulated significant amounts of long-chain PUFA. Compared to the results of hydrogenated marine samples, carbon number distributions of unhydrogenated TAG were shifted to the lower carbon number side, leading to biased carbon number patterns.

The bias in TAG carbon number distributions was confirmed through comparison with the mean chain length per fatty acid that was provided by FAME analysis. The mean chain length per fatty acid determined by neutral lipid profiles of unhydrogenated samples ($^1/_3$ of the mean acyl carbon number in TAG, expressed in mole %) was significantly lower than that determined by fatty acid analysis ($P < 0.05$). Samples with higher ratios in Figure 5 usually showed higher mean double bonds per fatty acid, but no linear correlation was found between them. The importance of polyunsaturation is shown by the large proportion of long-chain PUFA in these samples (Figure 6), especially the essential fatty acids, 20:5*n*-3 and 22:6*n*-3 in the neutral lipids. The highest ratio of hydrogenated to unhydrogenated neutral lipids in halibut eggs in Figure 5 coincides with their having the highest proportion of 22:6*n*-3 in fatty acids in the neutral lipid fraction (Figure 6). The high ratios in *Yoldia hyperborea* and *Nephthys ciliata* (Figure 5) were related to their having the largest proportion of PUFA, around 50% of their fatty acid composition, as well as the large proportion of 20:5*n*-3 in *Yoldia hyperborea* (Figure 6). One explanation for the high proportion of long-chain PUFA in the cold ocean species is that a greater amount of intracellular molecular oxygen is available at lower temperatures. This would be required by oxygen-dependent enzymes that catalyze the de-

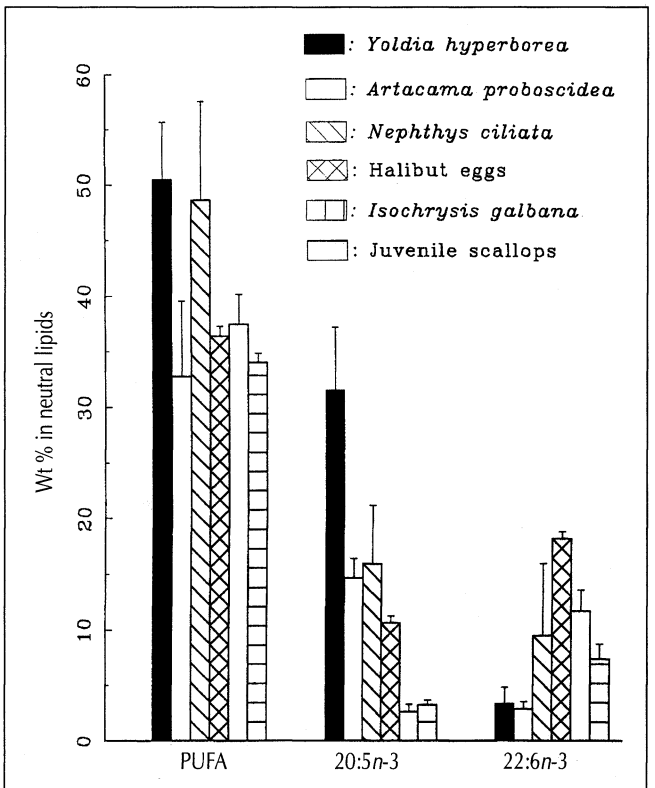

Figure 6. Percentage of total PUFA and major representatives in six kinds of marine species (mean ± standard deviation, $n \geq 3$, FAME analysis conditions as in the experimental section)

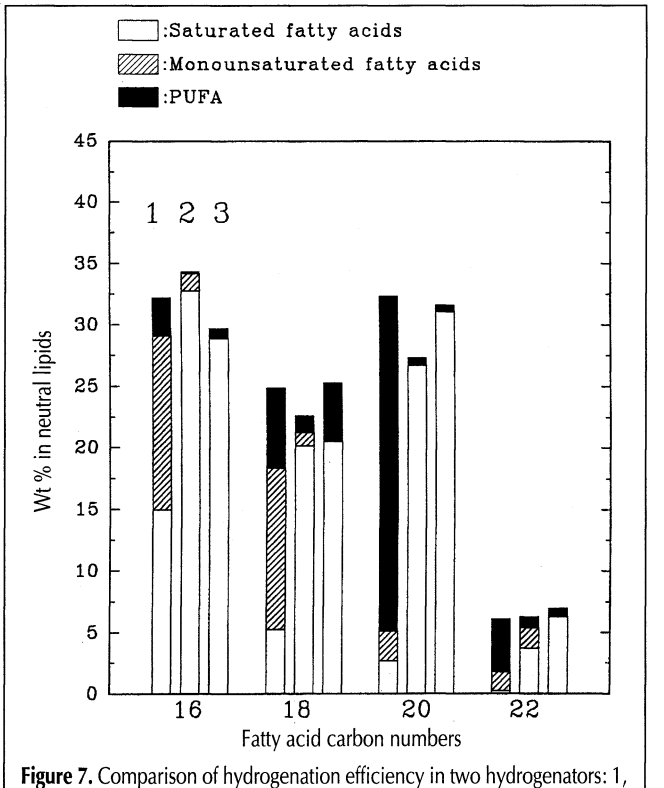

Figure 7. Comparison of hydrogenation efficiency in two hydrogenators: 1, without prehydrogenation; 2, hydrogenated with a simple homemade hydrogenator; and 3, with a commercial, atmospheric pressure hydrogenator ($n = 2$, FAME analysis conditions as in the experimental section).

saturation of long-chain PUFA (31). Also, unsaturated TAG may be more easily mobilized at subzero temperatures.

TAG with higher carbon numbers often have a greater degree of unsaturation and elute in a higher temperature region with a longer retention time and greater risk of decomposition or polymerization during GC analysis. Therefore, discrimination with respect to diverse degrees of unsaturation should be avoided during hydrogenation prior to GC analysis. Figure 7 shows that the hydrogenation efficiencies of two kinds of hydrogenators for the most highly unsaturated marine samples, *Y. hyperborea*, were almost identical, at approximately 90% ($P > 0.05$). Long-chain PUFA that contain up to six double bonds per fatty acid may be only partially hydrogenated (32). In contrast to the complicated single-sample operation of the commercial apparatus, the simple hydrogenation that was set up in our laboratory was rapid and allowed processing of several samples simultaneously. In addition to improving separations and ensuring sample stability, hydrogenation simplifies samples with different degrees of unsaturation and locations of double bonds to identical saturated ones so that a single f_W for each carbon number becomes practical (33).

Comparison of typical chromatograms of a bivalve, *Y. hyperborea*, with and without hydrogenation shows that hydrogenated sample peaks are sharper and narrower, and resolution is greatly improved (Figure 8). Small TAG peaks with odd and higher carbon numbers were readily distinguished from large peaks with even carbon numbers (Figure 8B). This is important for marine species because their neutral lipids seem to have wider carbon number distributions as compared with land-based animals, and some marine species contain moderate amounts of TAG with odd-numbered carbon (34). Peak broadening of natural TAG usually occurs on nonpolar columns as a result of a relatively early elution of the unsaturated compounds within a given carbon number. This does not allow true resolution of saturated and unsaturated species, but it may result in the overlap of different carbon numbers, especially if odd carbon number or branched-chain compounds are also present. Without hydrogenation, TAG that contained high proportions of PUFA exhibited peak shape distortion and tailing (Figure 8A), and small TAG peaks with odd or high carbon numbers were totally covered by major peaks with even carbon numbers.

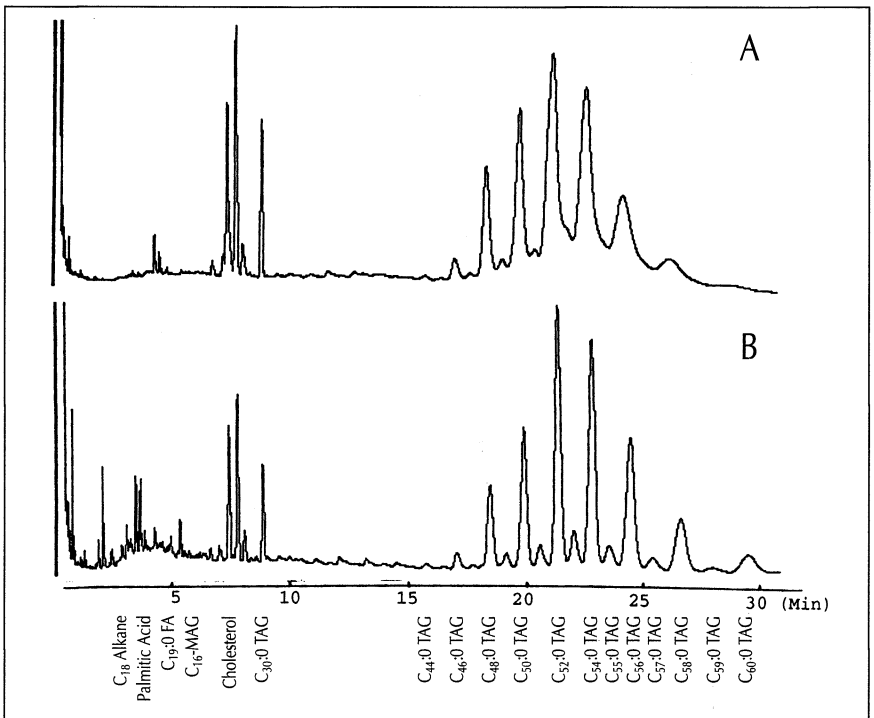

Figure 8. Chromatograms of neutral lipids from *Yoldia hyperborea*. (A) unhydrogenated, and (B) hydrogenated, at optimized conditions as listed in Figure 2 with helium as the carrier gas.

At the lower temperature zone of chromatograms, a better resolution of hydrogenated sterols in terms of carbon number was achieved in sea scallops which have a complex sterol composition (Figure 9). In humans, terrestrial animals, and fish, cholesterol is the principal sterol compound (>95% of the total). For this reason, most investigators may have focused on TAG in the high-temperature area in lipid profiles. However, 20 or more kinds of sterols with wide variations in concentration exist in some marine invertebrates. Complete separation of them requires a column length of up to 60 m and takes 2 h or more (35).

Unhydrogenated sterols resulted in overlapping peaks with the adjacent carbon numbers (Figure 9A) because of different side-chains, the various double bond locations, and the diverse degrees of unsaturation. For example, C_{27} sterols 22-dehydrocholesterol and desmosterol and C_{28} sterol brassicasterol, eluted at almost the same retention time between two standards, cholesterol and campesterol, even with a 30-m DB-5 column (36). In between these two saturated standards, cold water samples contained several sterols which could be identified as either C_{27} or C_{28}, depending on fluctuations in GC conditions. This indicated that carbon number profiles for scallop sterols were unreliable without hydrogenation. After hydrogenation, scallop sterols were grouped into three major peaks based on carbon numbers. Scallops probably contained small proportions of C_{26} and C_{30} sterols as well (37). The overlapping adjacent carbon number sterols in sea scallops, 22-dehydrocholesterol and brassicasterol, were hydrogenated to their saturated homologues, the former hydrogenated to the C_{27} standard, cholesterol, and the latter became campesterol. Three saturated standards, cholesterol, campesterol, and sitosterol, eluted at identical distances with baseline resolution as displayed in Figure 9B. Thus, correct evaluations of both sterol and TAG carbon number distributions in sea scallops were simultaneously achieved in a 28-min run. The carbon numbers of sterols in real samples were also confirmed through GC–MS of their TMS derivatives using a standard mass spectrum library.

Quantitative standards for complex lipids are normally not available. Therefore, the

analytical results of the complex lipid mixtures in the cold ocean samples were validated by another accepted chromatographic method, TLC–FID, which is a basic lipid-profiling method used in our laboratory (14). Since these two methods have different separation abilities, the sum of molecular species estimated by GC can be compared to the estimate for each neutral lipid subclass in TLC–FID analysis. In three marine invertebrates, summed molecular species from each major neutral lipid class were linearly correlated to the corresponding subclasses, TAG and sterols, determined by TLC–FID (Figure 10). A log–log plot was used for the TAG data as it ranged over two orders of magnitude, but the value of the slope indicated a linear relationship. The error bars for TLC–FID of sterols are slightly larger. This was similar to the comparison for plasma lipids (38).

Although complete hydrogenation causes the loss of double bonds in neutral lipid molecules, no information is lost in terms of lipid profiling because the GC method achieves separations based on carbon numbers. Furthermore, many marine species possess characteristic lipid compositions that can be recognized without complete resolution and determination of individual molecular species. Quantitative estimation of partially resolved lipid structures can be sufficient for establishing the origin of a neutral lipid extract and for evaluating physiological conditions of marine species. Some examples that employed the optimized high-temperature GC method follow.

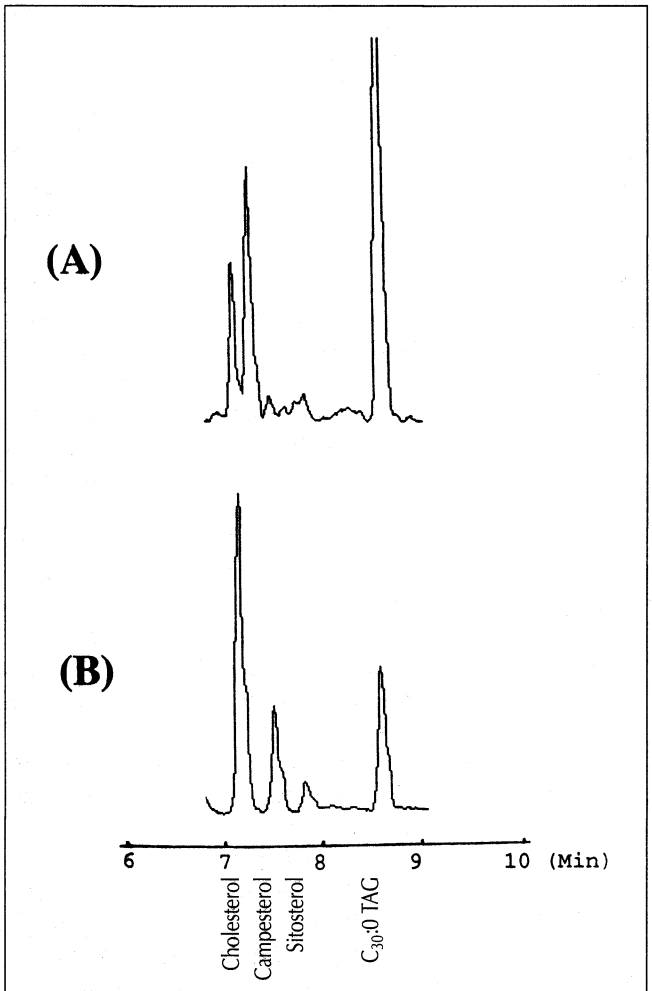

Figure 9. Effect of hydrogenation on sterol carbon number distributions in scallops (*Placopecten magellanicus*). (A) unhydrogenated, (B) hydrogenated (at optimized conditions as listed in Figure 2 with helium as the carrier gas). Note that different amounts of internal standard were added to each sample.

Applications

Cold water bivalves and polychaetes are part of the food web leading to cod and other predators. However, very little is known about the lipid composition of *Y. hyperborea* and the polychaetes, *N. ciliata* and *A. proboscidea.* Abundances and proportions of three major sterols in these invertebrates, C_{27}, C_{28}, and C_{29}, were very different (Figure 11B). C_{27} sterol was the most abundant in *N. ciliata*, followed by *A. proboscidea* and *Y. hyperborea,* respectively. Sterols regulate membrane functions, such as maintaining membrane fluidity, and act as precursors

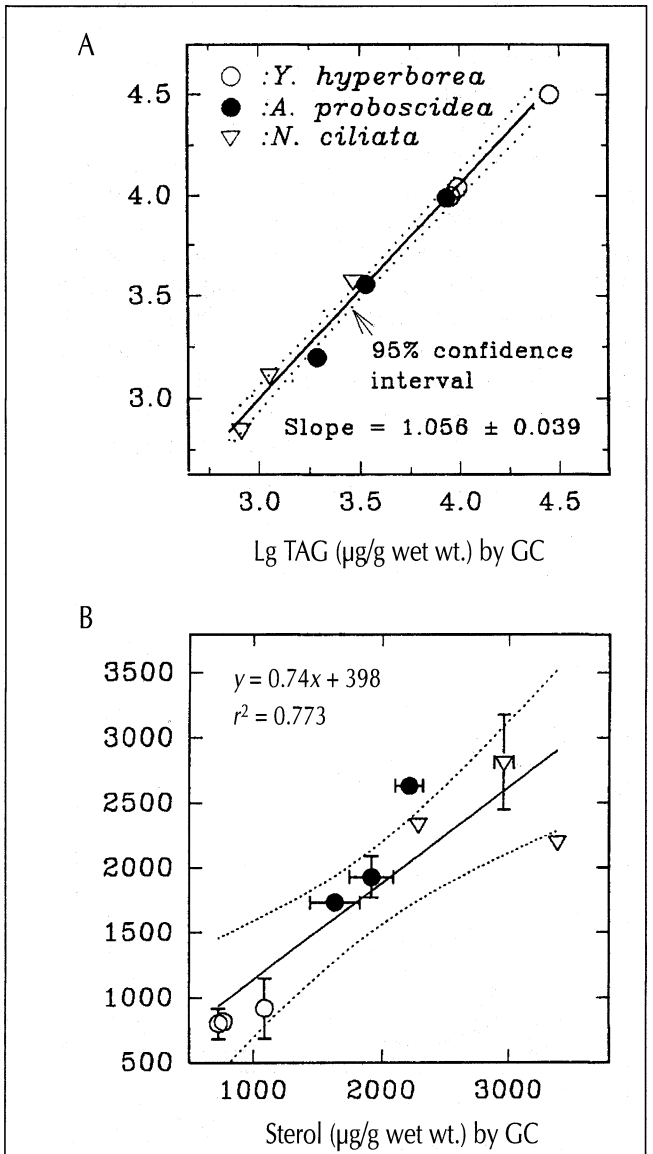

Figure 10. Correlation of neutral lipid amounts in three marine invertebrates analyzed by GC–FID and TLC–FID. (A) triacylglycerols, (B) sterols (mean ± standard deviation, $n = 2$, at optimized conditions as listed in Figure 2 with helium as the carrier gas).

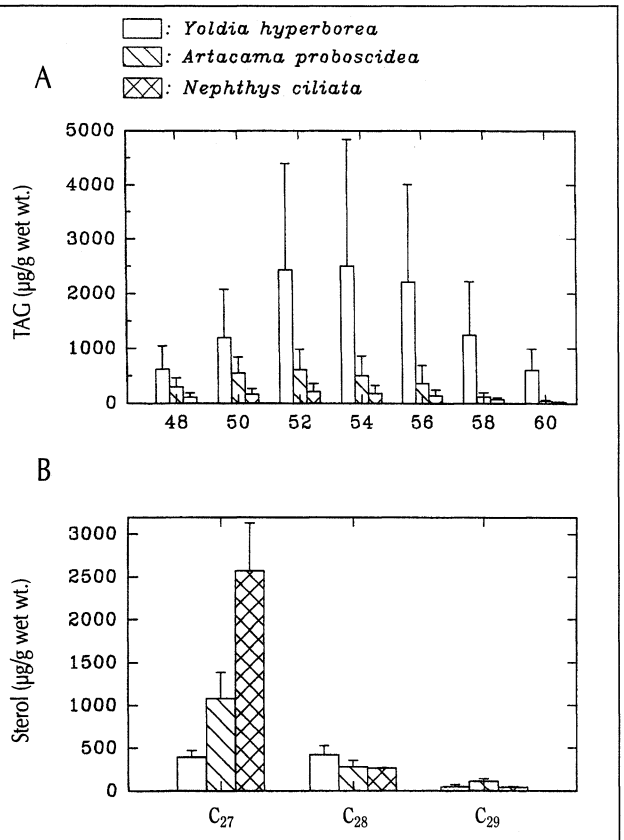

Figure 11. Absolute amounts of major neutral lipid compounds in three kinds of marine invertebrates. (A) triacylglycerols, (B) sterols (mean ± standard deviation, n = 3, at optimized conditions as listed in Figure 2 with helium as the carrier gas).

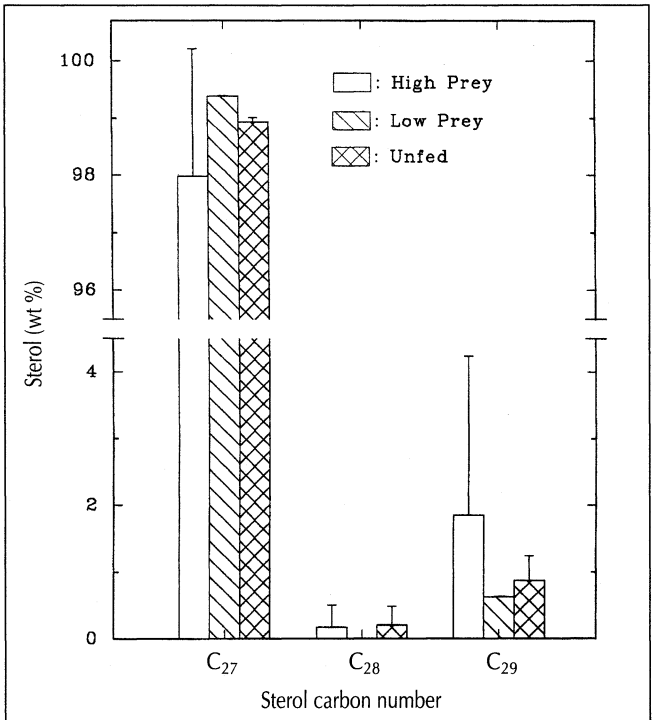

Figure 12. Carbon number distributions of sterols in neutral lipids of cod larvae (*G. morhua*) in feeding trials (mean ± standard deviation, n = 3, at optimized conditions as listed in Figure 2 with helium as the carrier gas).

for a range of metabolically active molecules. Sterols cannot be synthesized *de novo* from simple precursors by some invertebrates, so they rely on an external sterol supply (39). Although all three invertebrates were taken from the bottom of Conception Bay in Newfoundland, *Y. hyperborea* may selectively consume fresh phytoplankton, while the two burrowing polychaetes may consume detritus.

In most of the samples that were analyzed, the TAG carbon numbers ranged from 32 to 60. The three marine invertebrates showed similar symmetric carbon number distributions from 48 to 60 with an apex at 52 or 54. The highest amount of TAG (12.4 ± 9.8 mg/g wet wt) was found in *Y. hyperborea*, a threefold increase over the amount found in *A. proboscidea* (3.4 ± 2.5 mg/g) and a tenfold increase over that in *N. ciliata* (1.3 ± 0.9 mg/g) (Figure 11A). The mollusca store TAG as an energy source in many body components rather than in specific organs, as mammals do. The small amounts of TAG in *N. ciliata* may be due to the fact that fat is mainly deposited in its gut. There were much greater standard deviations in the concentrations of TAG compared with sterols in the three invertebrates, which may be the result of biological variation within each species, such as differences between sexes (40).

Quantitative measurement of the rates of ingestion and assimilation of nutrients from different prey taxa should advance our understanding of the feeding dynamics of early stage cod larvae. The carbon number distribution of sterols in cod larvae (*G. morhua,* Figure 12) was composed of approximately 99% C_{27} sterols; C_{28} sterols were almost absent, regardless of the variations in the three feeding experiments. In the larvae that were fed the high-prey diet, there were slightly lower levels of C_{27} (98%) and almost twice the amount of C_{29} sterols. There was also much greater variability in the sterol compounds from these larvae. This suggests that diet does influence sterol composition in cod larvae, but only to a small degree. This result is in accord with the literature (1): sterols in fish larvae usually resist diet manipulation, while TAG may readily be affected by feeding. Therefore, sterols may be useful in normalizing the TAG content to avoid size-specific variability.

These applications indicate that neutral lipid profiles by GC not only characterize carbon number patterns according to biological origins, but also differentiate the distributions within the same species which differ only in diet and physiological or environmental conditions.

Conclusion

Automated high-temperature GC on hydrogenated samples offers a precise tool for the measurement of highly unsaturated neutral lipid samples with acyl carbon numbers up to or slightly greater than 62. Sample hydrogenation allows for the correct evaluation of carbon number distributions in sterols and avoids discrimination in samples with high proportions of long-chain PUFA. In addition, use of large solvent plug sizes, fast injection rates, hydrogen as a carrier gas with high flow rates, and short capillary columns enhances recoveries of high molecular weight neutral lipids. With incorporation of these

procedures, neutral lipid carbon number profiles may be useful in defining physiological characteristics of diverse marine species.

By combining with dephosphorylation, this optimized GC method can be extended to analyze phospholipid moieties along with neutral lipids because there is enough room in the chromatograms to insert di- and monoacylglycerol peaks (19). Further study should verify the usefulness of the proposed method in samples that are rich in other lipid compounds, such as wax esters and hydrocarbons.

Acknowledgments

We thank J.S. Wells for technical assistance; J.A. Brown, R. J. Thompson, and P. Dabinett for providing marine samples; and R.W. Bishop, R.G. Norkus, and D.E. Willis for helpful reviews.

This paper was presented in part at the American Oil Chemists' Society annual meeting, Canadian section, October 1994, Winnipeg, Manitoba, Canada (O.S.C. contribution #269).

References

1. A.J. Fraser. Triacylglycerol content as a condition index for fish, bivalve, and crustacean larvae. *Can. J. Fish Aquat. Sci.* **46:** 1868–73 (1989).
2. A. Kuksis. Acylglycerols (glycerides). *CRC Handbook of Chromatography: Lipids,* Vol. I. H.K. Mangold, C. Zweig, and J. Sherma, Eds., CRC, Boca Raton, FL, 1984, pp. 381–480.
3. M. Goutx, C. Gerin, and T. Bertrand. An application of Iatroscan TLC with FID: Lipid classes of microorganisms as biomarkers in the marine environment. *Org. Geochem.* **16:** 1231–37 (1990).
4. E. Tvrzicka and P. Mares. Some limitations of plasma lipid analysis in clinical research by thin-layer chromatography with flame-ionization detection. *J. Chromatogr.* **530:** 424–31 (1990).
5. R.T. Crane, S.C. Goheen, E.C. Larkin, and G. Ananda. Complexities in lipid quantization using thin-layer chromatography for separation and flame ionization for detection. *Lipids* **18:** 74–80 (1983).
6. P. Mares. High-temperature capillary gas liquid chromatography of triacylglycerols and other intact lipids. *Prog. Lipid Res.* **27:** 107–33 (1988).
7. A. Staby, C. Borch-Jensen, S. Balchen, and J. Mollerup. Supercritical fluid chromatographic analysis of fish oils. *J. Am. Oil Chem. Soc.* **71:** 355–59 (1994).
8. P. Sandra, F. David, F. Munari, G. Mapelli, and S. Trestianu. HT–CGC and CSFC for the analysis of relatively high molecular weight compounds. *Supercritical Fluid Chromatography,* R.M. Smith, Ed. Royal Society of Chemistry, London, England, 1988, pp. 137–58.
9. A. Kuksis. GLC and HPLC of neutral glycerolipids. *Lipid Chromatographic Analysis,* T. Shibamoto, Ed. Marcel Dekker, New York, NY, 1994, pp. 177–222.
10. G. Holmer. Triglycerides. *Marine Biogenic Lipids, Fats, and Oils,* Vol. I. R.G. Ackman, Ed. CRC, Boca Raton, FL, 1989, pp. 139–73.
11. A. Kuksis, J.J. Myher, L. Marai, and K. Geher. Determination of plasma lipid profiles by automated gas chromatography and computerized data analysis. *J. Chromatogr. Sci.* **13:** 423–30 (1975).
12. J.J. Myher and A. Kuksis. Determination of plasma total lipid profiles by capillary gas–liquid chromatography. *J. Biochem. Biophys. Methods* **10:** 13–23 (1984).
13. E.G. Bligh and W.J. Dyer. A rapid method of total lipid extraction and purification. *Can. J. Biochem. Physiol.* **37:** 911–17 (1959).
14. C.C. Parrish. Separation of aquatic lipid classes by Chromarod thin-layer chromatography with measurement by Iatroscan flame-ionization detection. *Can. J. Fish Aquat. Sci.* **44:** 722–31 (1987).
15. A.I. Vogel. *Elementary Practical Organic Chemistry, Part III: Quantitative Organic Analysis.* Longman, London, 1958, pp. 763–65.
16. U. Olsson, P. Kaufmann, and B. Herslof. Multivariate optimization of a gas–liquid chromatographic analysis of fatty acid methyl esters of blackcurrant seed oil. *J. Chromatogr.* **505:** 385–94 (1990).
17. K. Grob. Injection techniques in capillary GC. *Anal. Chem.* **66:** 1009A–19A (1994).
18. K. Grob. Evaluation of injection techniques for triglycerides in capillary GC. *J. Chromatogr.* **178:** 387–92 (1979).
19. A. Kuksis and J.J. Myher. Gas chromatographic analysis of plasma lipids. *Adv. in Chromatogr.* **28:** 267–332 (1989).
20. M.S. Klee. *GC Inlets - An Introduction.* Hewlett-Packard, Palo Alto, CA, 1990, pp. 14–16.
21. K. Grob and H.P. Neukom. Factors affecting the accuracy and precision of cold on-column injections in capillary gas chromatography. *J. Chromatogr.* **189:** 109–17 (1980).
22. P. Mares and P. Husek. Quantitative capillary gas-liquid chromatography of triglycerides on a fused-silica column with a chemically bonded stationary phase. *J. Chromatogr.* **350:** 87–103 (1985).
23. J.V. Hinshaw and L.S. Ettre. Aspects of high-temperature capillary gas chromatography. *HRC&CC* **12:** 251–54 (1989).
24. C. Litchfield, R.G. Ackman, J.C. Sipos, and C.A. Eaton. Isovaleroyl triglycerides from the blubber and melon oils of the beluga whale (*Delphinapterus leucas*). *Lipids* **6:** 674–81 (1971).
25. P. Mares, E. Tvrzicka, and J. Skorepa. Automated quantitative gas–liquid chromatography of intact lipids II: Accuracy, precision and reproducibility of results. *J. Chromatogr.* **164:** 331–43 (1979).
26. S. Falk-Petersen, J.R. Sargent, and K.S. Tande. Lipid composition of zooplankton in relation to the sub-arctic food web. *Polar Biol.* **8:** 115–20 (1987).
27. J.T. Scanlon and D.E. Willis. Calculation of flame ionization detector relative response factors using the effective carbon number concept. *J. Chromatogr. Sci.* **23:** 333–40 (1985).
28. P. Mares, J. Skorepa, E. Sindelkova, and E. Tvrzicka. Gas–liquid chromatographic analysis of intact long-chain triglycerides. *J. Chromatogr.* **273:** 172–79 (1983).
29. P. Mares. The GLC of plasma intact lipids in clinical research. *Chromatography of Lipids in Biomedical Research and Clinical Diagnosis,* A. Kuksis, Ed. Elsevier, Amsterdam, 1987, pp. 128–62.
30. I.S. Gilkison. Quantitative capillary GC of triglycerides using a polarizable stationary phase. *HRC&CC* **12:** 481–83 (1989).
31. C.M. Brown and A.H. Rose. Fatty-acid composition of *Candida utilis* as affected by growth temperature and dissolved-oxygen tension. *J. Bacteriol.* **99:** 371–78 (1969).
32. H.B.W. Patterson. *Hydrogenation of Fats and Oils.* Applied Science, London, England, 1983, pp. 7–10.
33. W.W. Christie. *Gas Chromatography and Lipids, a Practice Guide.* Oily Press, Ayr, Scotland, 1989, pp. 192–93.
34. C. Litchfield, R.D. Harlow, and R. Reiser. Gas–liquid chromatography of triglyceride mixtures containing both odd and even carbon number fatty acids. *Lipids* **2:** 363–70 (1967).
35. G.E. Napolitano, B.A. MacDonald, R.J. Thompson, and R.G. Ackman. Lipid composition of eggs and adductor muscle in giant scallops (*Placopecten magellanicus*) from different habitats. *Mar. Biol.* **113:** 71–76 (1992).
36. P.W. Albro, J.L. Schroeder, and J.T. Corbett. Lipids of the earthworm *Lumbricus terrestris. Lipids* **27:** 136–143 (1992).
37. D.R. Idler and P. Wiseman. Molluscan sterols: a review. *J. Fish Res. Bd. Canada* **29:** 385–98 (1972).
38. P. Mares, M. Ranny, and J. Sedlacek. Chromatographic analysis of blood lipids: Comparison between gas chromatography and thin-layer chromatography with flame ionization detection. *J. Chromatogr.* **275:** 295–305 (1983).
39. E. Tsitsa-Tzardis, G.W. Patterson, G.H. Wikfors, P.K. Gladu, and D. Harrison. Sterols of *Chaetoceros* and *Skeletonema. Lipids* **28:** 465–67 (1993).
40. P. Lubet, G. Brichon, J.Y. Besnard, and G. Zwingelstein. Sexual differences in the composition and metabolism of lipids in the mantle of the mussel *Mytilus galloprovincialis* LMK (Mollusca: bivalvia). *Comp. Biochem. Physiol.* **84B:** 279–85 (1986).

Manuscript accepted July 31, 1996.